International Journal of Mass Spectrometry 277 (2008) 123–129

Contents lists available at ScienceDirect

International Journal of Mass Spectrometry

journal homepage: www.elsevier.com/locate/ijms

Electron attachment studies to musk ketone and high mass resolution anionic isobaric fragment detection

A. Mauracher[a], P. Sulzer[a], E. Alizadeh[a], S. Denifl[a], F. Ferreira da Silva[a], M. Probst[a], T.D. Märk[a], P. Limão-Vieira[b], P. Scheier[a,*]

[a] Institut für Ionenphysik and Angewandte Physik, Center of Molecular Biosciences Innsbruck, Universität Innsbruck, Technikerstraße 25, A-6020 Innsbruck, Austria
[b] Atomic and Molecular Collisions Laboratory, CEFITEC, Departamento de Física, Universidade Nova de Lisboa, 2829-516 Caparica, Portugal

ARTICLE INFO

Article history:
Received 10 April 2008
Received in revised form 2 June 2008
Accepted 9 June 2008
Available online 18 June 2008

We dedicate this paper to Prof. Eugen Illenberger, not only a renowned scientist but also a loyal colleague and a trusted friend, on the occasion of his 65th birthday.

Keywords:
Electron attachment
Musk ketone
Nitro aromatic compound

ABSTRACT

Gas phase electron attachment studies have been performed for musk ketone by means of a crossed electron–molecular beams experiment in an energy range from 0 to 15 eV with a resolution of ~70 meV. Additional measurements, utilizing a two-sector-field instrument, have been used to distinguish between possible isobaric products. Anion efficiency curves for 19 anions have been measured including a long-lived (metastable) non-dissociated parent anion which is formed at energies near 0 eV. Many of the dissociative electron attachment products observed at low energy arise from surprisingly complex reactions associated with multiple bond cleavages and structural and electronic rearrangement. The present results are compared with previous aromatic nitrocompounds studied in our laboratory recently. Particularly the close similarity of musk ketone and the explosive trinitrotoluene is of special interest.

© 2008 Elsevier B.V. All rights reserved.

1. Introduction

Musk ketones (structure see Fig. 1) are one of the important classes of nitro aromatic compounds that have been widely used in the production of fragrances and other house holding applications such as air fresheners and cleaners. As far as health is concerned, humans are at risk from synthetic musk fragrances not only through their exposure from contaminated food species, but also through direct absorption through the skin from the many household sources of (musk) fragrances. Synthetic musk fragrances have been found in human body fat, with nitro-musks found more in women than men; some synthetic musks get passed to breast-feeding babies in breast milk [1], although its toxicity is still a matter of debate and not completely tested. Nitrocompounds are also found as important raw materials and products of the chemical industry and particularly in the production of explosives, pesticides and drugs (see e.g., [2]). Therefore, identification of musk containing products is essential as far as explosive detection is concerned.

High electron energy resolution electron attachment experiments on trinitrotoluene (TNT, structure see Fig. 1) and on three isomers of di-nitrobenzene (DNB) have been recently performed by Sulzer et al. [3,4]. It was found that these compounds form long-lived molecular anions and also undergo dissociative electron attachment (DEA) resulting preferentially in the formation of NO_2^-. These studies have also permitted to consider the potential of NO_2^- to serve as a fingerprint for the identification of the neutral compound, especially because resonant EA cross-sections have revealed to be unique for every molecular target. The potential of DEA to identify different structural isomers by recording the ion yield curves of the various fragments was recently demonstrated in the case of the three isomers of nitrotoluene (NT) [5].

In the present experiments we investigate the negative ion formation in musk ketone at low electron energies (0–15 eV) by recording the ion yield curves with a high electron energy resolution. We find that, at all energies, by far the dominant signal is due to NO_2^-. This is in striking contrast to other aromatic nitrocompounds, where it was found that formation of the non-decomposed parent anion at low energy is the dominant signal [4,5]. In musk ketone the parent anion is also formed, but with a comparably low intensity.

2. Experimental

We have performed dissociative electron attachment experiments to musk ketone utilizing two different apparatus in our

* Corresponding author. Fax: +43 512 507 2932.
E-mail address: Paul.Scheier@uibk.ac.at (P. Scheier).

1387-3806/$ – see front matter © 2008 Elsevier B.V. All rights reserved.
doi:10.1016/j.ijms.2008.06.006

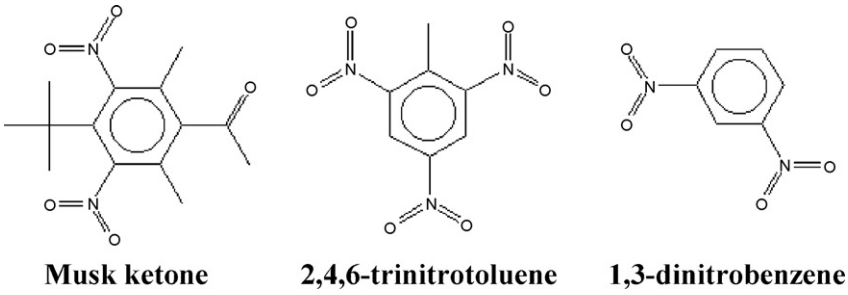

Fig. 1. Molecular structures of musk ketone, 2,4,6-TNT and 1,3-DNB.

laboratory to investigate negative ion resonances under high electron energy resolution (70 meV) and high-mass resolution (up to $m/\Delta m \sim 3000$).

2.1. Hemispherical electron monochromator

Electron attachment to musk ketone was investigated by means of a crossed electron–molecular beams set-up which has been described in detail elsewhere [5]. Briefly, a high resolution, 70 meV (FWHM), electron beam is formed in a hemispherical electron monochromator with typical currents of ≈5 nA. Negative ions formed in the interaction region are mass analyzed by means of a quadrupole, and mass-selected negative ions are detected by a channel electron multiplier operated in the pulse counting mode. The intensity of a particular mass-selected negative ion is obtained as a function of the electron energy.

2.2. High mass resolution sector-field

A two-sector-field mass spectrometer equipped with a standard Nier-type ion source was used in the present studies [6]. The electron beam was guided by a homogeneous magnetic field of about 20 mT. This field is sufficiently high to prevent extraction of electrons from the ion source. The electron current passing through the ion source block was set to 10 μA and this value was reached at an electron energy of about 4 eV. Thus, the anion yield at lower electron energies may be different compared to the partial cross-section. Since at these low electron energies the electron current entering the ion source region is likely to be much larger than the trap current measured at the Faraday cup, a correction of the relative cross-sections cannot be made. At electron energies below 4 eV we recommend only the data from the monochromator instrument. The electron energy resolution close to 0 eV was estimated from the width of the SF_6^-/SF_6 signal to be ∼1 eV. The anionic species formed were pushed by a repeller lens out of the interaction region and accelerated by a voltage drop of 6 kV to the analyzing section of the mass spectrometer. After mass selection in the magnetic sector-field the ions pass a 1.48 m long field-free region and enter the electrostatic sector-field. Except for a few masses the mass resolution was kept at a value of about $m/\Delta m = 1000$. The anions are detected with a channel electron multiplier from Dr. Sjuts Optotechnik GmbH operated in a pulse counting mode. Complete negative ion mass spectra of musk ketone have been recorded for several electron energies. Furthermore, anion efficiency curves are measured for 19 selected anions in the mass spectra by measuring the ion yield as a function of the electron energy from about 0 to 15 eV.

In both set of experiments, musk ketone was purchased from Fluka with a minimum stated purity of 97% and used as delivered. Musk ketone is solid at room temperature and therefore has to be heated in order to increase the vapor pressure so that at moderately elevated temperatures (between 60 and 90 °C, well below the melting point) an effusive molecular beam can be generated. For the present working temperatures we expect no thermal decomposition of the molecules. The electron energy scales are calibrated using the well-known SF_6^-/SF_6 signal near 0 eV.

3. Results and discussion

3.1. Negative ion mass spectrum

All mass spectra in Fig. 2 were measured with the hemispherical monochromator instrument. Fig. 2 (upper diagram) shows a negative ion mass spectrum of musk ketone obtained by summation of individual mass spectra measured at several different electron energies, i.e., from an electron energy close to 0 up to 10 eV in 1 eV steps. From this data it is possible to get an overview of all possible fragments. For a mass spectrum recorded at one energy only those anions that are produced within one resonance can

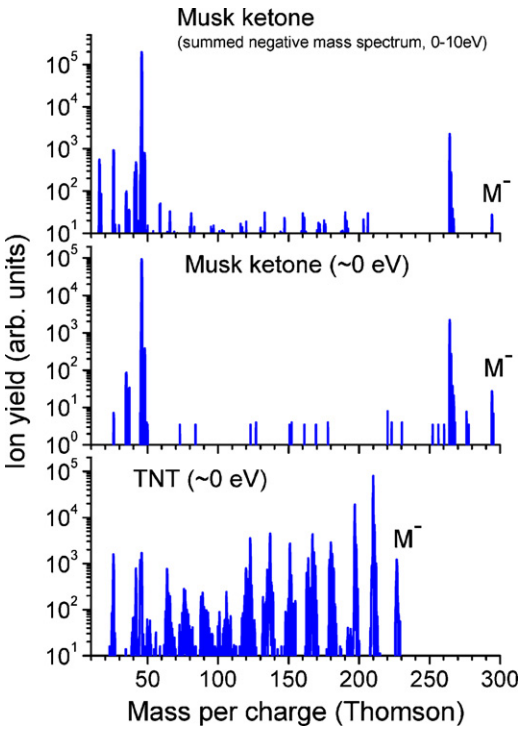

Fig. 2. Anion mass spectra of musk ketone and TNT measured with the monochromator instrument. The upper diagram shows a mass spectrum derived upon summation of 11 individual mass spectra measured upon DEA to musk ketone at electron energies from ∼0 to 10 eV. The two lower diagrams show anion mass spectra of musk ketone (middle diagram) and TNT (lower diagram and taken from Ref. [3]) measured close to 0 eV.

be identified. The fragmentation patterns observed have been classified into four different groups according to their ionic yields: (a) NO_2^- fragment is by far the dominant anion followed by the 264 amu fragment that is formed by the loss of NO and assigned as $[M-NO]^-$; (b) the second group includes the species 42, 26 and 16 amu which can be assigned to fragment ions $C_2H_2O^-$, CN^- and O^-, respectively; (c) the third comprises masses 294, 248, 206 and 59 amu which have been identified as the metastable parent anion M^{*-}, $[M-NO_2]^-$, $[M-2NO-CO]^-$ and $CHNO_2^-$, respectively; (d) the masses 81 and 160 amu are identified as $C_5H_5O^-$ and $[M-CH_3-CH_3CO-NO_2-NO]^-$ anions, respectively. Fig. 2 shows the mass spectrum of musk ketone obtained at 0 eV (middle diagram), which can be compared to the mass spectrum of TNT obtained at the same electron energy (lower diagram). As in the case of TNT [3] musk ketone shows a surprisingly rich fragmentation pattern for electron energies close to 0 eV, and a weak formation of the metastable parent anion. This is in striking difference to other nitrocompounds, like nitrobenzene [7] and nitrotoluene [5] where the yield for the parent anion at the 0 eV resonance is large. The two mass spectra measured close to 0 eV indicate a rich chemistry driven upon low-energy electron attachment to TNT and musk ketone. Thermo-chemical calculations indicate that most of the low mass fragments cannot be formed close to 0 eV. However, rearrangement of the neutral fragments and the formation of highly stable neutral fragments may give an explanation. This is discussed in more detail at the section of different anionic species.

A geometry optimization of 2,4-DNT [8] as a model system with two nitrogroups, one *ortho* and one *para* to the methyl group, was carried out at the Hartree–Fock level with Dunning's correlation consistent valence triple zeta basis set (cc-pVTZ). One could observe that the oxygen atoms of the nitro group at position 2, *ortho* to the methyl group, are moved out of the plane of the benzene ring and the nitrogen atom. Compared to the planar structure, the oxygen atom closer to the methyl group is rotated by 26.5° around the C–N axis, while the other one is rotated by 25.7°. The nitro group at position 4 remains in plane with the atoms of the benzene ring. For musk ketone a similar rotation of the nitro groups can be expected which will affect the DEA cross-sections as demonstrated for the isomers of NT [5] and DNB [3]. *Ab initio* calculations performed for the three isomers of di-nitrobenzene [4] suggest two low lying anionic states associated with extended wave functions for the extra electron which were reported to be delocalized over the ring and the two NO_2 groups. Further to this, Sulzer et al. [3] have assigned the low lying electronic states (below 1 eV) in electron attachment to TNT to be due to shape resonances with the extra electron delocalized over the ring and the three nitro groups. Therefore, bearing in mind the electron affinities of the nitro group and the acetyl radical (C_2H_3O) are 2.27 and 0.42 eV, respectively [9], it is reasonable to characterize the low-energy features for musk ketone to shape resonances as well.

3.2. Ion efficiency curves

The formation of the non-dissociated parent ion is just restricted to a narrow feature close to 0 eV (Fig. 3, obtained with the monochromator instrument), while all other fragment ions show more extended resonance profiles indicative of DEA. Within the variety of resonant structures in the entire energy range from 0 to 15 eV the anion intensity of most of the fragments is concentrated within three main areas, in the range below 1, 3–7 and 7–12 eV. While the TNIs generated at low energy (<1 eV) are assigned as shape resonances involving the π^* antibonding orbitals, it is likely that the resonance features at higher energies can be characterized as core-excited resonances with possible contributions of high-energy shape resonances.

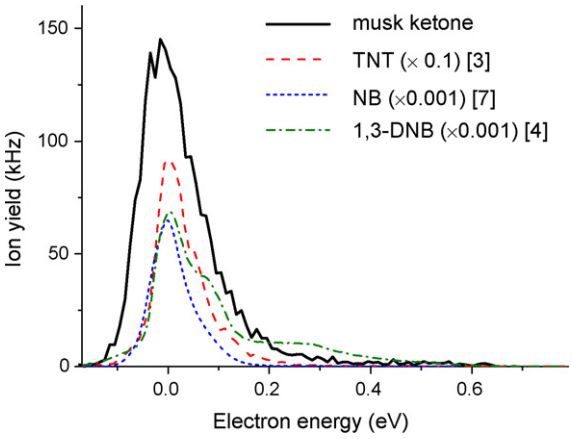

Fig. 3. Anion efficiency curves for the parent molecular anions of several nitro aromatic compounds measured under similar conditions (electron energy resolution $\Delta E \sim 70$ meV, electron current, neutral particle density). Please note the different intensities obtained for the four molecules differ by almost three orders of magnitude.

3.2.1. Parent molecular anion (associative attachment) $M^-/C_{14}H_{18}N_2O_5^-$ (294 amu)

The ~0 eV resonant structure for the non-dissociated parent molecular ion integrates only to a comparatively weak feature with respect to the abundant ion signals resulting from dissociative electron attachment. This is in contrast to other nitrocompounds such as TNT [3], nitrotoluene [5], di-nitrobenzene [4] and nitrobenzene [7] where the relative intensity of the parent anion is much larger. The parent anions of these nitro aromatic compounds are also shown in Fig. 3. The width of the musk ketone parent anion peak is determined as 130 meV and essentially is due to the limited resolution in these experiments, with a non-symmetric profile towards higher energies. Electron attachment at these low energies yielding the formation of a non-dissociated molecular ion comprises the energy of the incoming electron and the electron affinity of the molecule, which may result in a statistical intramolecular rearrangement delaying autodetachment [10].

3.2.2. The complementary ions NO_2^- (46 amu) and $[M-NO_2]^-/C_{14}H_{18}NO_3^-$ (248 amu)

These ions are formed via the cleavage of one of the two C–N bonds leading to the complementary DEA reactions as follows:

$$e^- + M \leftrightarrow (M)^{\#-} \rightarrow [M-NO_2] + NO_2^- \quad (1a)$$

$$e^- + M \leftrightarrow (M)^{\#-} \rightarrow [M-NO_2]^- + NO_2 \quad (1b)$$

Reaction (1a) is endothermic with a thermodynamic threshold at 0.83 eV as calculated from the bond dissociation energy taken from the average value in nitrocompounds, $D(C-NO_2) = 3.1$ eV [11], and the well-known electron affinity, $EA(NO_2) = 2.27$ eV [9]. Therefore, the formation of NO_2^- ion at low electron energy around 0 eV is energetically not allowed. The experimental appearance energy of this fragment is below the calculated threshold, which may indicate that electron attachment proceeds through vibrationally excited states (hot bands) even though the number density of such hot molecules at room temperature may be low. Indeed such hot band transitions for DEA at low energies have been reported in the past (see e.g.,Refs. [7,12,13] and references therein). A second more favorable explanation is the rearrangement of the neutral product into more stable species. A close inspection of the low-energy resonance of NO_2^- reveals two structures (see insert in Fig. 4) at ~0.11 and 0.29 eV that we tentatively assign to the activation of the symmetric stretching vibrational mode of NO_2 with an energy of 0.163 eV [14]. The dashed line shows the anion efficiency curve

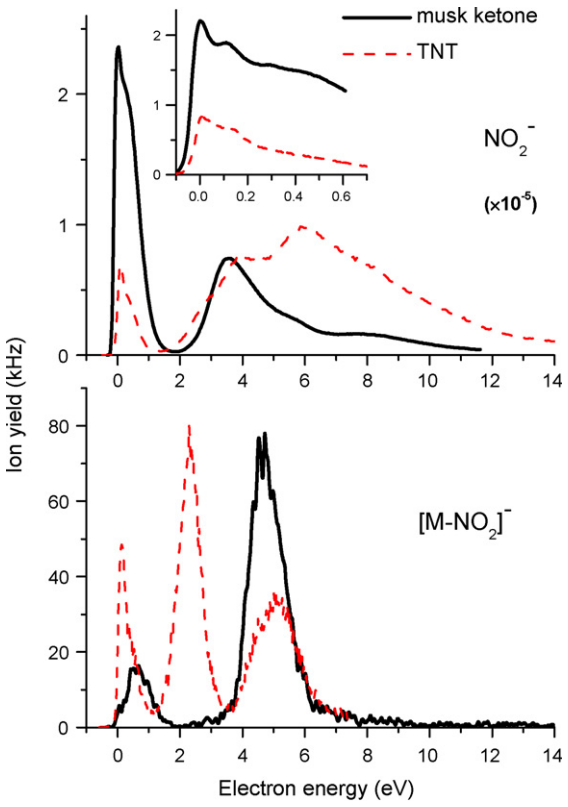

Fig. 4. Anion efficiency curves for NO_2^- (upper diagram) and $[M-NO_2]^-$ (lower diagram) formed upon DEA to musk ketone (solid lines) and 2,4,6-TNT (dashed lines and taken from [3]) measured with high electron energy resolution.

of NO_2^- formed upon DEA to TNT taken from Ref. [3]. The positions of all resonances are almost identical for the two molecules, however, the relative intensities of the resonances differ strongly. Thus high resolution DEA can be used as a very powerful method to distinguish the two compounds. The high-energy resonances (Table 1) are certainly due to core-excited resonances (Fig. 4 (upper diagram)).

When comparing the energy region between the signal from NO_2^- (Fig. 4, (upper diagram), obtained with the monochromator instrument) and its complementary ion $[M-NO_2]^-$ (Fig. 4, (lower diagram), obtained with the monochromator instrument), the former extends to much higher energies indicating that this may be related to a possible distribution of the excess energy within the dissociating system. If we assume a statistical behavior in the unimolecular decomposition of the transient negative ion, the large fragment may take about 97% of the available excess energy due to the large number of vibrational degrees of freedom. At high electron energies the internal energy of the heavy neutral fragment formed via reaction (1a) will lead to the decomposition into lower mass neutrals, which does not affect the observed anionic channel NO_2^-. In contrast, for reaction (1b) high internal energy stored in the heavy anionic product will lead to decomposition into lower mass anions and thus limits the observation of $[M-NO_2]^-$ to lower electron energies compared to reaction NO_2^-.

3.2.3. *Loss of neutral NO units $[M-nNO]^-$, n = 1, 2*

The ionic yield of the fragment ion due to the loss of a neutral NO, $C_{14}H_{18}NO_4^-$, is plotted in Fig. 5 (obtained with the monochromator instrument) with a steep onset at zero energy. In the isomers of DNB [4] it was also observed but at resonant features generally speaking above 0.5 eV (with the exception of 1,4-DNB), while for TNT [3] we observe the same behavior. It is particular interesting that the loss of an NO radical can actually be triggered by an excess electron at just 0 eV. $[M-NO]^-$ shows a resonant feature (Table 1) at ~0.1 eV that can be related to the symmetric stretching vibrational excitation of the molecular anion that still keeps an NO_2 group intact (with an excitation energy of 0.163 eV as reported before). This seems reasonable, since the loss of an NO group should not affect the delocalization of the charge over the whole molecule. Indeed, the *ab initio* calculations of Sulzer et al. [4] have shown that the extra charge on the low lying anionic states of di-nitrobenzene remains

Table 1
Peak positions for the fragment ions of musk ketone obtained in the present experiments

Mass (Da)	Anionic species	Peak position (eV)								
294	M^-	~0	–	–	–	–	–	–	–	–
264	$[M-NO]^-$	~0	~0.1	–	–	–	–	–	~9.3	–
252	$[M-CNO]^-$	~0	–	–	3.0	–	–	8.0	–	–
250	$[M-NO_2]^-$	~0	–	–	3.5	5.5	–	8.5	–	–
249	$[M-NO_2]^-$	~0	–	–	3.5	5.5	–	8.5	–	–
248	$[M-NO_2]^-$	~0	~0.1	~0.3	3.5	5.5	–	8.5	–	–
234	$[M-2NO]^-$	~0	–	–	~3.0	6.0	–	–	9.0	–
231	$[M-NO_2-OH]^-$	~0	–	–	~3.5	6.0	–	–	9.0	–
222	$[M-CNO-NO]^-$	~0	–	–	3.5	–	7.5	–	–	–
218	$[M-NO_2-NO]^-$	~0	–	–	3.5	–	–	8.0	–	–
206	$[M-2NO-CO]^-$	–	–	–	3.5	–	–	8.5	–	–
160	$[M-2(CH_3)CO_2(NO)_2]^-$	–	–	–	–	5.0	–	–	9.0	10.0
81	$C_5H_5O^-$	–	–	–	–	5.0	–	–	9.0	10.0
59	$CHNO_2^-$	–	–	–	4.0	6.0?	–	8.5	–	10.0
51	$^{13}CC_3H_2^-$	0	–	–	3.5	5.5	–	8.5	–	10.0
50	$C_4H_2^-$	0	–	–	3.5	5.5	–	8.5	–	10.0
48	$^{14}N^{16}O^{18}O^-$	~0	0.11	0.29	3.5	5.5	–	8.5	–	–
47	$^{15}NO_2^-$	~0	–	–	3.5	5.5	–	8.5	–	–
46	$^{14}NO_2^-$	~0	0.11	0.29	3.5	5.5	–	8.5	–	–
43	$^{13}C^{12}CH_2O^-$	~0.5	–	–	4.0	–	6.5	8.5	–	–
42	$C_2H_2O^-$	~0.5	–	–	4.0	–	6.5	8.5	–	–
27	$^{13}CN^-$	~0	–	–	4.5	5.5	–	8.0	–	–
26	CN^-	~0	–	–	4.5	5.5	–	8.0	–	–
18	$^{18}O^-$	~0	–	–	–	6.0	–	–	9.0	–
16	$^{16}O^-$	~0	–	–	–	6.0	–	–	9.0	–
1	H^-	~0	–	–	–	5.0	–	–	9.5	–

(?) means peak position uncertain.

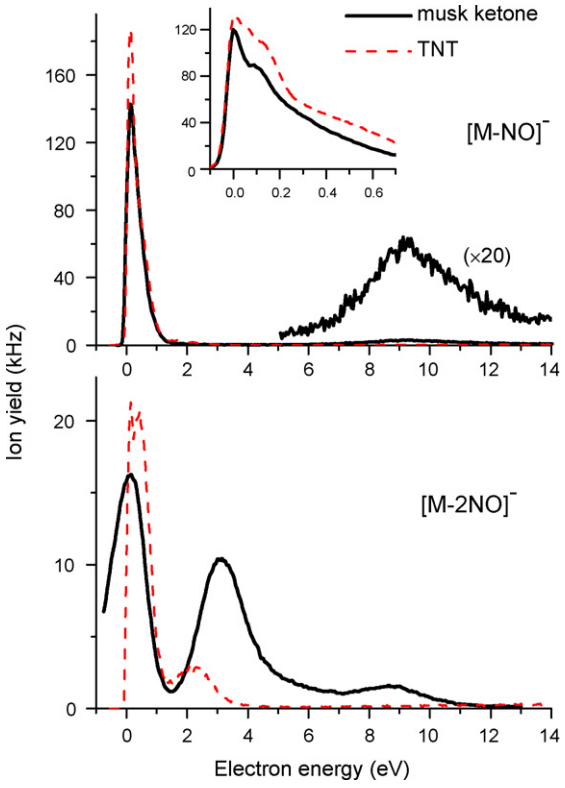

Fig. 5. Anion efficiency curves for $[M–NO]^-$ (upper diagram) and $[M–2NO]^-$ (lower diagram) formed upon DEA to musk ketone (solid lines) and 2,4,6-TNT (dashed lines and taken from [3]). All anions except $[M–2NO]^-$ from musk ketone were measured with high electron energy resolution. The latter one was measured with the sector-field instrument and an electron energy resolution of about 1 eV.

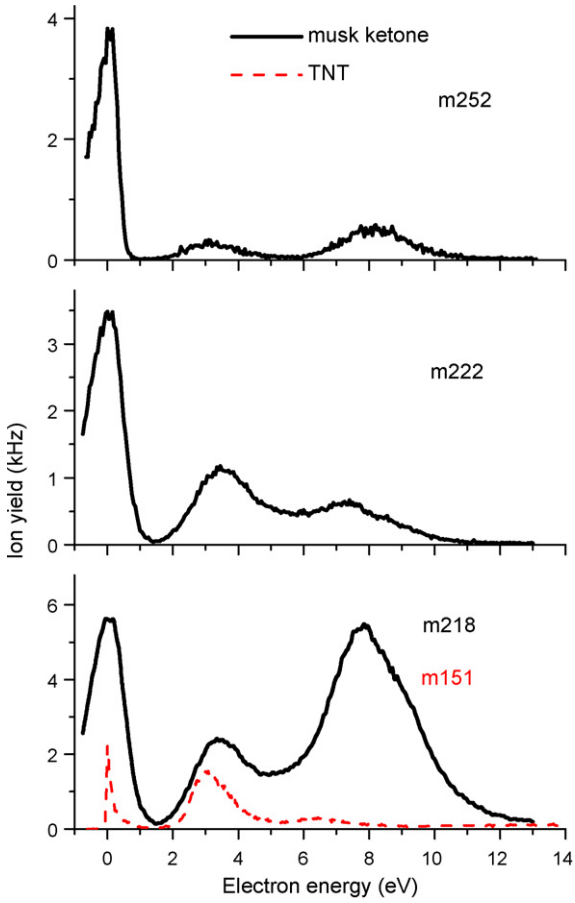

Fig. 6. Anion efficiency curves for $[MCNO]^-$ (mass 252 amu, upper diagram), $[MCNO-NO]^-$ (mass 222 amu, middle diagram) and $[MNO_2–NO]^-$ (mass 218 amu, lower diagram) formed upon DEA to musk ketone (solid lines) and 2,4,6-TNT (dashed line and taken from [3]). All anions from musk ketone were measured with the sector-field instrument and an electron energy resolution of about 1 eV. The anion with a mass of 151 amu formed upon DEA to TNT was measured with the electron monochromator instrument and an electron energy resolution of better than 100 meV.

delocalized over the benzene ring and the two NO_2 groups. The structures of the final neutral and ionic products remain unknown. The sequential loss of two neutral NO fragments was observed as delayed unimolecular decomposition in the two field-free regions of the mass spectrometer [8]. The corresponding parent anion $M^{\#-}$ was formed at an electron energy close to 0 eV. The relatively high abundance of this channel suggests that sequential NO loss is also operative in the ion source and can be assigned to the formation of the anion with a mass of 60 amu below the parent molecular anion.

3.2.4. $[M–CNO]^-$ (252 amu), $[M–CNO–NO]^-$ (222 amu) and $[M–NO_2–NO]^-$ (218 amu)

The resonant structures of these fragment anions are shown in Fig. 6 (the solid curves are obtained with the sector-field instrument, the dashed curve is obtained with the monochromator instrument) with their energy positions listed in Table 1. The shape and position of the resonance features for $[M–CNO]^-$, $[M–CNO–NO]^-$ and $[M–NO_2–NO]^-$ are very similar, which indicates that these anions have common precursor transient anion states. The resonances observed at 8.0 eV (Table 1) can also be assigned to electronically excited TNI states (including Rydberg excitation), which may decompose via one fragment anion plus one or more neutrals.

3.2.5. Ion yield (206 amu), $[M–2NO–CO]^-/C_{13}H_{18}O_2^-$

The anion efficiency curve of the fragment ion with a mass of 206 amu is plotted in Fig. 7 (obtained with the monochromator instrument) and shows one strong resonant feature peaking at ~3.5 eV and a weak and diffuse structure at 8.5 eV. These resonances can be assigned to electronically excited TNI states (including Rydberg), which may then decompose via one anion and several neutral fragments. $C_{13}H_{18}O_2^-$ ion formation most probably proceeds via the following reaction:

$$e^- + M \rightarrow (M)^{\#-} \rightarrow [M–2NO–CO]^- + 2NO + CO \quad (2)$$

where the formation of $N_2 + O_2$ is energetically more favorable than two NO radicals, according to Table 2. However, delayed fragmentation of nitro aromatic compounds exhibit a sequential loss of NO [8]. The 206 amu yields a structure with a stoichiometric composition $C_{13}H_{18}O_2^-$, which may represent the 2,5,5-trimethyl-2-phenyl-1,3-

Table 2
Gas phase standard heats of formation (ΔH_f°) and electron affinities relevant in dissociative electron attachment to musk ketone (taken from Ref. [9])

Compound	ΔH_f° (kJ mol^{-1})
NO_2	33.1
N_2O_3 (dinitrogentrioxide, ONNOO)	82.84
CN	435.14
Compound	**Electron Affinity (eV)**
NO_2	2.273 ± 0.005
CN	3.862 ± 0.005
CNO	3.609 ± 0.005

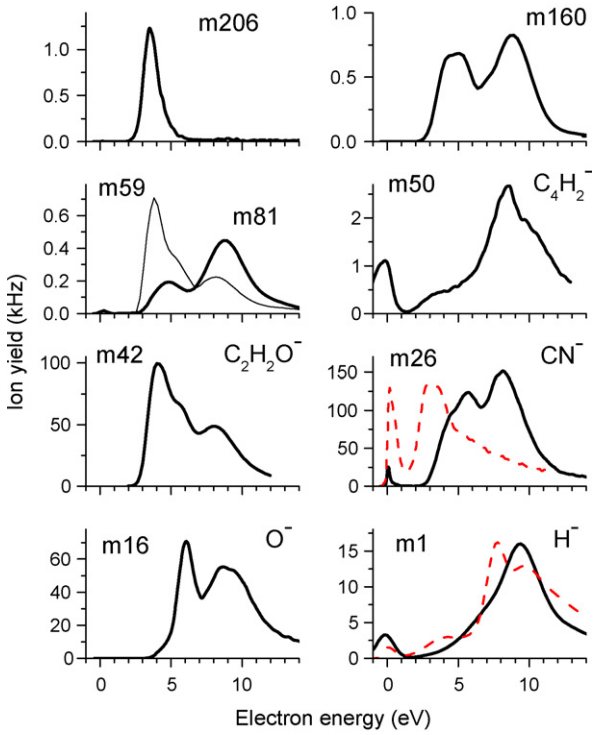

Fig. 7. Anion efficiency curves for fragments formed upon DEA to musk ketone (solid lines) and TNT (dashed lines, CN^- taken from [3]). All anions except $C_4H_2^-$ and H^- (for both molecules) were measured with high electron energy resolution. H^- and $C_4H_2^-$ were measured with the sector-field instrument and an electron energy resolution of about 1 eV.

dioxane anion. The value $\Delta_f H_g^\circ$ ($C_{13}H_{18}O_2^-$) is not known and therefore it is impossible to compute the thermodynamic threshold of reaction (2) producing $C_{13}H_{18}O_2^-$.

3.2.6. Low intensity ion yields of $C_{11}H_{12}O^-$ (160 amu), $C_5H_5O^-$ (81 amu) and $CHNO_2^-$ (59 amu)

Formation of a set of fragment ions with low intensities is shown in Fig. 7 (obtained with the monochromator instrument) and the peak positions are listed in Table 1. A close inspection of the ionic yields reveals the presence of resonant features in two energy regions, 3–7 and 7–12 eV. Possible assignments for these ions are: at 160 amu, 2-phenylbicyclo(1,1,1)pentane-2-ol which may be formed from musk ketone by the loss of $2(CH_3) + CO_2 + 2(NO)$; for 81 amu, the 2-furanyl-CH_2 anion and for 59 amu, the $CHNO_2$ radical anion. The formation of these molecular ions may involve the cleavage of several bonds and a series of intramolecular rearrangements. In fact, such an assumption is reinforced from the presence of the low lying anionic state at a threshold near 3 eV, which can also suggest that high-energy resonances may consist of two electrons in normally unoccupied molecular orbitals moving in the field of the positive core, therefore accounting for core-excited resonances. Moreover, as far as $CHNO_2^-$ ion is concerned, we have reported recently its formation from nitromethane [15,16] where it may result from an electronically excited TNI (including Rydberg excitation). The resonance positions may suggest that these anions may have common precursor transient anion states.

3.2.7. Ion yields of $C_4H_2^-$ (50 and 51 amu)

The present measurements yielding $C_4H_2^-$ show five resonances (Table 1). The formation of this anion requires complex rearrangements in the precursor ion involving several bond breakings. All nitrogen and oxygen atoms are part of the neutral products and in the case of the low-energy structure recorded close to 0 eV they have to form highly stable molecules such as N_2, CO_2 or H_2O to compensate for the energy required to break all these bonds. The calculated isotopic ratio between 51 and 50 amu for C_4H_2 is 4.1% and the measured ratio is 4.4%.

3.2.8. Ion yields of $C_2H_2O^-$ (42 and 43 amu)

The present experiments yielding a fragment ion with mass 42 amu (Fig. 7) indicate that this anion is $C_2H_2O^-$. The anion efficiency curve of mass 43 amu has the same shape and its yield is 2.2% of the anion yield of mass 42. This has also been verified with a mass scan for this fragment and its isotope with high-mass resolution at an electron energy of 4 eV. The calculated isotopic ratio between 43 and 42 for $C_2H_2O^-$ is 2.2% whereas the calculated isotopic ratio for CNO^- is 1.5% which does not match the experiment. However, recent dissociative electron attachment experiments to three isomers of di-nitrobenzene [4] assigned mass 42 as CNO^-. This radical is known to have a pseudohalogen character and with an electron binding energy of 3.61 eV [12]. The present finding questions the previously assigned structure for mass 42 since no isotopic checks were made.

3.2.9. CN^- (26 and 27 amu) formation

The DEA cross-sections for CN^- and $^{13}CN^-$ formation are shown in Fig. 7 (obtained with the monochromator instrument) and the estimated positions for the resonances are presented in Table 1. The intensity ratios ^{12}C:^{13}C are approximately 1.5% matching very well the natural abundance of such isotopes. The cyanide anion CN^- represents an excision of this unit from the target molecule. CN is a well-known pseudohalogen having an appreciable electron affinity (3.862 eV, Table 1) exceeding even that of the halogen atoms. Formation of CN^- via complex DEA reactions is well-known in amino acids and other larger molecules containing C and N atoms [6,17].

The resonance features for CN^- formation in TNT from Sulzer et al. [3] can be compared with the present results of musk ketone as far as using DEA as a method to distinguish chemical compounds with similar structures.

3.2.10. $^{16}O^-$ and $^{18}O^-$ formation

DEA leading to the formation of $^{16}O^-$ and $^{18}O^-$ was measured and the curve for ^{16}O is shown in Fig. 7 (obtained with the monochromator instrument). The peak positions are listed in Table 1. As far as cross-section values for $^{18}O^-$ formation are concerned, the 6.0 and 9.0 eV resonances are within the expected isotopic ratio of 1:500 with respect to the $^{16}O^-$ formation.

3.2.11. H^- formation

The partial cross-section for the DEA reaction channel $H^-/C_{14}H_{18}N_2O_5$ is shown in Fig. 7 (measured with the sector-field instrument) and the resonance structure position is listed in Table 1. The spectrum shown in Fig. 7 represents the recorded H^- signal obtained by subtracting the background signal (with a pressure of 10^{-5} Pa) from the sample signal (at a working pressure of 3×10^{-4} Pa). The dashed line in the lower, left diagram of Fig. 7 shows the anion efficiency curve of H^- formed upon DEA to TNT. For energies in the vicinity of electronically excited states of the neutral molecule, fragmentation most likely originates from a core-excited resonance, consisting of two electrons in normally unoccupied MOs moving in the field of the positive core. The structures observed for H^- (~6 and 8 eV) (Fig. 7 and Table 1) are signatures of core-excited resonances initiated via probably ($\sigma \rightarrow \pi^*$) and ($\pi \rightarrow \pi^*$) electron transitions. If we take D(C—H) = 4.5 eV [14] and EA(H) = 0.75 eV, the

threshold for H^- formation is 3.75 eV which is above the observed value, meaning that simple bond cleavage will not lead to the formation of the hydride anion at electron energies below 3.73 eV (the same is true also for TNT). The most likely explanation for H^- formation at low energies is a substantial energy gain upon decomposition and rearrangement of the neutral products into stable molecules such as N_2, CO_2 and H_2O.

4. Conclusions

The present DEA studies to musk ketone show partial cross-sections measured in the electron energy range of 0–15 eV with: (a) an electron high resolution of ~70 meV in a crossed electron–molecular beam set-up equipped with an hemispherical electron monochromator and (b) a two-sector-field mass spectrometer equipped with a standard Nier-type ion source with a energy resolution of ~1 eV. Capture of an excess electron with virtually no energy by musk ketone shows very particular features as far as the parent molecular anion is concerned, and also a variety of DEA products is produced. The formation of the parent anion occurs over a very narrow energy range near 0 eV with DEA reactions leading to several other anionic fragments in this same energy range. The DEA mechanism extends also to higher energies involving different resonant features. In comparison with other nitrocompounds the cross-section for the formation of the parent anion is relatively weak. This can be explained by the competition of the different DEA channels that are already operative near zero energy. The most dominant DEA reaction is the formation of NO_2^-. Further and more complex reactions are observed like the loss of up to two neutral NO units having a steep onset at zero energy.

Due to the resonant nature of DEA processes, the relative attachment cross-sections characteristics are unique for every molecule and so DEA experiments have shown to be a powerful technique to identify small traces of chemically similar compounds, as is the case of TNT and musk ketone. Therefore this technique has revealed also to be a fingerprint in future sensing and field explosive detection instrumentation.

Acknowledgments

This work has been supported by the Fonds zur Förderung der wissenschaftlichen Forschung (FWF), Wien, the European Commission, Brussels, via ITS-LEIF, EIPAM and ECCL networks. PLV acknowledges ECCL COST-CM0601 support for the short-term scientific mission to Innsbruck. S.D. acknowledges an APART-fellowship from the Austrian Academy of Sciences.

References

[1] B. Liebl, S. Ehrenstorfer, Chemosphere 27 (1993) 2253.
[2] R.N. Compton, L.G. Christophorou, G.S. Hurst, P.W. Reinhardt, J. Chem. Phys. 45 (1966) 4634.
[3] P. Sulzer, F. Rondino, S. Ptasinska, E. Illenberger, T.D. Märk, P. Scheier, Int. J. Mass Spectrom. 272 (2008) 149.
[4] P. Sulzer, A. Mauracher, S. Denifl, M. Probst, T.D. Märk, P. Scheier, E. Illenberger, Int. J. Mass Spectrom. 266 (2007) 138.
[5] P. Sulzer, A. Mauracher, S. Denifl, F. Zappa, S. Ptasinska, M. Beikircher, A. Bacher, N. Wendt, A. Aleem, F. Rondino, S. Matejcik, M. Probst, T.D. Märk, P. Scheier, Anal. Chem. 79 (2007) 6585.
[6] D. Huber, M. Beikircher, S. Denifl, F. Zappa, S. Matejcik, A. Bacher, V. Grill, T.D. Märk, P. Scheier, J. Chem. Phys. 125 (2006) 084304.
[7] A. Pelc, P. Scheier, T.D. Märk, Vacuum 81 (2007) 1180.
[8] A. Mauracher, S. Denifl, M. Probst, T.D. Märk, P. Scheier, (2008) submitted to publication.
[9] NIST Chemistry webbook: http://webbook.nist.gov/chemistry.
[10] E. Illenberger, in: C.-Y. Ng (Ed.), Advanced Series in Physical Chemistry, vol. 10B, World Scientific, Singapore, 2000, pp. 1063–1160.
[11] T.B. Brill, K.J. James, Chem. Rev. 93 (1993) 2667.
[12] S. Gohlke, A. Rosa, F. Brüning, M.A. Huels, E. Illenberger, J. Chem. Phys. 116 (2002) 10164.
[13] I. Bald, I. Dabkowska, E. Illenberger, O. Ingólfsson, Phys. Chem. Chem. Phys. 9 (2007) 2983.
[14] D.A. Lide (Ed.), Handbook of Chemistry and Physics, 78th ed., CRC Press, Boca Raton, 1997.
[15] W. Sailer, A. Pelc, S. Matejcik, E. Illenberger, P. Scheier, T.D. Märk, J. Chem. Phys. 117 (2002) 7989.
[16] E. Alizadeh, F. Ferreira da Silva, F. Zappa, A. Mauracher, M. Probst, S. Denifl, A. Bacher, T.D. Märk, P. Limão-Vieira, P. Scheier, Int. J. Mass Spectrom 271 (2008) 15.
[17] P. Papp, J. Urban, S. Matejcik, M. Stano, O. Ingólfsson, J. Chem. Phys. 125 (2006) 204301.